NUCLEOTIDE REGULATION OF THE STRUCTURE AND DYNAMICS OF G-ACTIN

MARISSA G. SAUNDERS, JEREMY TEMPKIN, JONATHAN WEARE, AARON R. DINNER, BENOÎT ROUX, AND GREGORY A. VOTH

SUPPLEMENTARY TEXT

METHODS

SYSTEM SET-UP FOR 2D UMBRELLA SAMPLING

These structures were solvated by first including all the non-overlapping crystal structure waters from 1NWK and 1ATN after aligning each subdomain independently. In addition, the water molecules around the active site Mg^{2+} cation were placed into form a hexacoordinated structure around the cation when including the oxygen atoms from the β and γ phosphates of the nucleotide. The backbone, nucleotide, cation, and 1^{st} solvation shell around the cation were constrained to their starting positions with a spring constant of 10 kcal/mol while the waters from the crystal structure and the sidechains were constrained to their starting positions with a spring constant of 1 kcal/mol. The water molecules were minimized for 5K steps, the non-water molecules were minimized for 5K steps, and then all atoms were minimized for 10K steps. While maintaining constraints, the system was heated to 310 K over 1 ps and then pre-equilibrated for 1 ns while releasing the constraints in a stepwise manner.

RMSD CALCULATION WITHIN EACH CG SITE

The C_α RMSD was calculated using the average structure over the 4 ns of production simulation in the lowest energy window of each system during 2D US. Two different reference structures were used – the average structure from G-ADP and the average from Oda-ADP. For each reference structure, the RMSD of the 4 ns trajectory from the average structure is given in the bolded columns of SI Table 2. This represents the expected variation based on thermal fluctuations. In all other columns, the RMSD of one average structure to the reference structure is given.

ERROR ESTIMATION

Error estimation is in the form value ± standard error of the mean (SEM). To evaluate the SEM, we made the conservative assumption that every 200 ps of simulation represented an independent sample.

RESULTS AND DISCUSSION

COMPARISON BETWEEN THE STABILIZED ODA STATE AND THE PREVIOUSLY REPORTED 'SUPER-CLOSED' STATE

A previously published paper (1) reported two findings which on face seem very similar to the findings in this work, but which upon closer examination are actually fundamentally

different. Splettstoesser et al reported the observation of a super-closed, putatively polymerization-competent configuration of monomeric actin in ATP-bound G-actin that was not seen in ADP-bound G-actin. Based on the existence of this alternate state, they noted that the average cleft width in ATP-bound actin was smaller than that in ADP-bound actin. In the current paper, however, we see two non-converting conformations: the G-actin and Oda conformations. In the minimum energy conformation of both these states we observe a nucleotide-dependent shift in the cleft width (see Table S2 and Fig 2).

As we have addressed in a previous paper (2), the findings in the Splettstoesser et al paper are similar to what we observe when the nucleotide cleft is not pre-solvated with waters from the crystal structure and with hexacoordinated waters around the calcium at the cleft of the actin molecule. This poorly equilibrated starting condition manifests in a dynamic instability during minimization that leads to a divergence in the simulations to the superclosed and open states. The fact that the Splettstoesser et al paper reports observing multiple transitions from the G-actin configuration to the 'super-closed' configuration within 4 nanoseconds in a series of unbiased MD simulations in and of itself fundamentally is contradictory to the findings in both our previous and current papers. As reported previously, when we preserve the crystal structure solvation in the nucleotide cleft we observe no flattening of the actin molecule. Even with significant applied bias in the 2D umbrella sampling of the current work, there is no transition on the timescales that we could simulate to the Oda-like conformation from the properly solvated G-actin structure (note each of our windows was 4 ns in length, and because of the umbrella sampling algorithm those windows furthest from the starting point represent approximately 28 ns of simulation (7 temporally contiguous windows)).

In addition to the differences in energetics and conversion rates between the phenomena that we describe and the "superclosed" state of the Splettstoesser paper, there are structural differences. The two nucleotide-dependent differences in hydrogen bonding that are provided in the Splettstoesser et al paper are the interactions between the nucleotide and either Gly301 (where hydrogen bonding is observed only ~20% of the time in ADP-bound simulations but 70% of the time in ATP-bound simulations) or Lys336 (where ATP forms a hydrogen bond 65% of the time in ATP-bound actin but not at all in ADP-bound actin). It is not mentioned in the Splettstoesser paper what criteria was used for hydrogen bonding, but the closest contact distance between the nucleotide tail and these residues reveals clear differences from the Splettstoesser results. As shown in SI Table 3, in our simulations the nucleotide tail is consistently within 3.3 Å of residue 301 regardless of conformation or nucleotide. Conversely, there is no hydrogen bonding between Lys336 and the nucleotide tail it our simulations – the average minimum contact distances for all conformations/nucleotides are greater than 3.9 Å. We would regard any contact between Lys336 and the nucleotide as a significant deviation from either the Oda model or the crystal structures, in which the closest contact between the phosphate tail and Lys 336 are 3.9, 5.1, and 4.6 Å for the 2ZWH (Oda), 1NWK (ATP G-actin) and 1J6Z (ADP G-actin) structures respectively.

SUPPLEMENTARY FIGURES AND TABLES

Table S1: Protein residues in each CG site

CG site number	Residues
1	5 to 33, 80 to 147, 334 to 349
2	34 to 39, 52 to 69
3	148 to 179, 273 to 333
4	180 to 219 252 to 262
5	40 to 51
6	236 to 251
7	263 to 272
8	350 to 375
9	Nucleotide and cation
10	1 to 4
11	70 to 79
12	220 to 235

Table S2: Collective variable values for the initial structures and the minimum energy configurations observed in both the 1D and 2D umbrella sampling simulations.

	GADP	GATP		OADP		OATP		
Initial Structure								
PDB ID	1J6Z	1NWK		2ZWH		2ZWH		
2-1-3-4 dihedral angle (degrees)	-26.3	-26.6		-6.9		-6.9		
2-4 distance (angstroms)	23.7	24.7		20.7		20.7		
1D Umbrella Sampling								
2-1-3-4 dihedral angle (degrees)	-23.9	-27.4*	-23.9	-19.9	-12.9*	-21.9*	-18.1*	-7.4
2D Umbrella Sampling								
2-1-3-4 dihedral angle (degrees)	-26.25	-22.75		-8.25		-6.25		
2-4 distance (angstroms)	24.9	24.5		21.9		21.1		

* indicates the lowest energy minima

Table S3: Based on the C_α RMSD between average structures for the lowest energy window in each of the systems simulated, the internal structure of the CG sites does not change significantly upon either changing the nucleotide or changing the starting configuration.

	G-ADP reference				O-ADP reference			
	G-ADP[a]	G-ATP[b]	O-ADP[b]	O-ATP[b]	G-ADP[c]	G-ATP[c]	**O-ADP**[a]	O-ATP[c]
SD1	**0.5**	0.5	0.7	0.9	0.7	0.6	**0.5**	0.7
SD2	**0.4**	0.4	0.7	0.5	0.7	0.5	**0.6**	0.5
SD3	**0.5**	0.5	0.8	0.5	0.8	0.6	**0.5**	0.8
SD4	**0.4**	0.5	0.9	0.9	0.9	1.2	**0.4**	0.7

a. RMSD (Å) from average during 4 ns of simulation; b. RMSD (Å) of average structure to the G-ADP average structure; c. RMSD (Å) of average structure to the O-ADP average structure.

Table S4: The main coarse-grained sites are reoriented and repositioned relative to one another in response to either changes in nucleotide or changes in the starting configuration. The first site in each pair is the reference site; the second is the comparison site (see text for more details).

	G-ADP:G-ATP	O-ADP:O-ATP	G-ADP:O-ADP	G-ATP:O-ATP
Difference in CG distance (Å)				
1-2	-0.05 ± 0.02	-0.49 ± 0.02	0.32 ± 0.02	-0.12 ± 0.01
1-3	-0.17 ± 0.01	0.04 ± 0.01	-0.08 ± 0.01	0.13 ± 0.01
3-4	0.02 ± 0.01	-0.22 ± 0.01	0.27 ± 0.01	0.02 ± 0.01
4-2	1.03 ± 0.02	0.961 ± 0.02	3.16 ± 0.02	3.09 ± 0.02
Difference in center of mass position given reference alignment (Å)				
1-2	1.13 ± 0.02	1.39 ± 0.02	1.56 ± 0.03	2.22 ± 0.03
3-1	1.52 ± 0.03	0.79 ± 0.02	1.25 ± 0.02	1.50 ± 0.03
3-4	0.90 ± 0.02	1.40 ± 0.02	2.16 ± 0.03	1.07 ± 0.02
4-2	4.05 ± 0.07	1.71 ± 0.03	10.08 ± 0.05	7.14 ± 0.04
Angle between the 3rd moments of inertia (degrees)				
1-2	10.6 ± 0.3	21.2 ± 0.6	15.0 ± 0.5	21.8 ± 0.5
3-1	7.5 ± 0.2	6.1 ± 0.1	6.1 ± 0.1	12.8 ± 0.2
3-4	5.0 ± 0.1	4.7 ± 0.1	10.3 ± 0.1	6.7 ± 0.1
4-2	14.0 ± 0.3	21.8 ± 0.6	23.3 ± 0.8	39.6 ± 0.5

Table S5: Comparison of distances between key residues between CG sites in the G- and Oda states. For each pair, the average distance ± the standard error of the closest contact between the two residues is given. All distances are measured in angstroms.

	G-actin, ADP	G-actin, ATP	Oda, ADP	Oda, ATP
Between CG sites 1 and 3				
72-158	2.88 ± 0.07	5.16 ± 0.07	5.1 ± 0.1	5.11 ± 0.09
73-158	3.5 ± 0.2	2.7 ± 0.1	2.8 ± 0.1	3.0 ± 0.1
73-159	2.64 ± 0.06	2.41 ± 0.07	3.0 ± 0.1	2.8 ± 0.1
74-158	5.3 ± 0.1	5.5 ± 0.1	3.5 ± 0.1	3.00 ± 0.09
74-159	3.1 ± 0.1	4.0 ± 0.1	2.5 ± 0.06	3.4 ± 0.1
109-161	2.65 ± 0.06	4.3 ± 0.2	2.60 ± 0.05	2.41 ± 0.05
109-163	2.38 ± 0.05	2.33 ± 0.05	2.51 ± 0.07	5.1 ± 0.1
110-172	2.9 ± 0.1	2.55 ± 0.09	4.1 ± 0.3	6.6 ± 0.2
110-175	2.25 ± 0.05	2.53± 0.09	3.0 ± 0.2	2.9 ± 0.2
375-169	5.0 ± 0.4	2.7± 0.1	3.4 ± 0.3	14.2 ± 0.5
Between CG sites 2 and 4				
59-207	5.2 ± 0.2	3.3 ± 0.2	4.4 ± 0.2	2.4 ± 0.2
62-203	2.8 ± 0.1	2.67 ± 0.09	6.1 ± 0.2	5.41 ± 0.06
62-205	8.9 ± 0.2	6.9 ± 0.2	5.2 ± 0.2	1.78 ± 0.04
62-207	6.7 ± 0.2	2.4 ± 0.2	4.4 ± 0.3	3.16 ± 0.08
62-244	16.0± 0.4	13.2 ± 0.4	4.4 ± 0.6	5.6 ± 0.2
69-207	9.4 ± 0.2	7.5 ± 0.3	1.75 ± 0.03	1.9 ± 0.1
Between CG sites 3 and 4				
157-210	5.6 ± 0.1	4.6 ± 0.1	1.92 ± 0.08	4.80 ± 0.08
207-210	1.74± 0.02	1.86 ± 0.07	1.73 ± 0.02	1.75 ± 0.02

Table S6: Comparison of distances between key residues in actin and the nucleotide or magnesium for the G- and Oda states. For each pair given, the average distance ± the standard error of the closest contact between the two residues is given. All distances are measured in angstroms.

	G-actin, ADP	G-actin, ATP	Oda, ADP	Oda, ATP
Ntd/MG-11	4.20 ± 0.07	5.87 ± 0.05	3.95 ± 0.04	4.03 ± 0.04
Ntd/MG-12	5.60 ± 0.05	5.05 ± 0.05	5.63 ± 0.04	5.27 ± 0.06
Ntd/MG-13	2.44 ± 0.04	2.50 ± 0.04	2.45 ± 0.04	2.50 ± 0.03
Ntd/MG-14	2.16 ± 0.06	1.81 ± 0.03	1.84 ± 0.04	1.74 ± 0.02
Ntd/MG-15	2.57 ± 0.1	2.11 ± 0.04	1.99 ± 0.04	1.98 ± 0.04
Ntd/MG-16	2.68 ± 0.1	2.00 ± 0.04	2.15 ± 0.08	2.03 ± 0.04
Ntd/MG-33	5.34 ± 0.09	5.10 ± 0.07	5.12 ± 0.08	4.71 ± 0.06
Ntd/MG-71	6.65 ± 0.06	4.91 ± 0.07	5.40 ± 0.09	5.00 ± 0.07
Ntd/MG-73	7.71 ± 0.1	5.27 ± 0.1	8.61 ± 0.1	6.44 ± 0.1
Ntd/MG-74	6.45 ± 0.09	4.79 ± 0.08	6.10 ± 0.1	4.21 ± 0.08
Ntd/MG-154	4.03 ± 0.04	4.39 ± 0.05	4.14 ± 0.06	4.12 ± 0.03
Ntd/MG-156	2.61 ± 0.04	2.45 ± 0.03	2.71 ± 0.05	2.58 ± 0.03
Ntd/MG-157	2.18 ± 0.05	2.16 ± 0.04	2.78 ± 0.07	2.09 ± 0.04
Ntd/MG-158	3.47 ± 0.05	1.86 ± 0.03	3.83 ± 0.09	2.21 ± 0.08
Ntd/MG-159	4.70 ± 0.05	2.75 ± 0.06	4.82 ± 0.07	3.63 ± 0.06
Ntd/MG-301	2.85 ± 0.05	3.28 ± 0.06	2.77 ± 0.05	2.94 ± 0.05

Figure S1: A) The correlation between the slowest mode in a trajectory made up of concatenating the G-actin (green) and Oda configurations (red) for the dihedral angles surrounding the G-like (-27.25 to-25.25) and Oda-like (-7.25 to -5.25) states in the ADP and ATP-bound simulations. B) the corresponding simulation is projected onto only the slowest mode and representative configurations from the G-actin (pink) and Oda (blue) halves of the constructed trajectories are shown. The 2-4 distance is given in angstroms. C) Over the first four modes, the average mode value only differs significantly between configurations for the first mode, indicating that of these modes only the first adequately distinguishes between configurations .

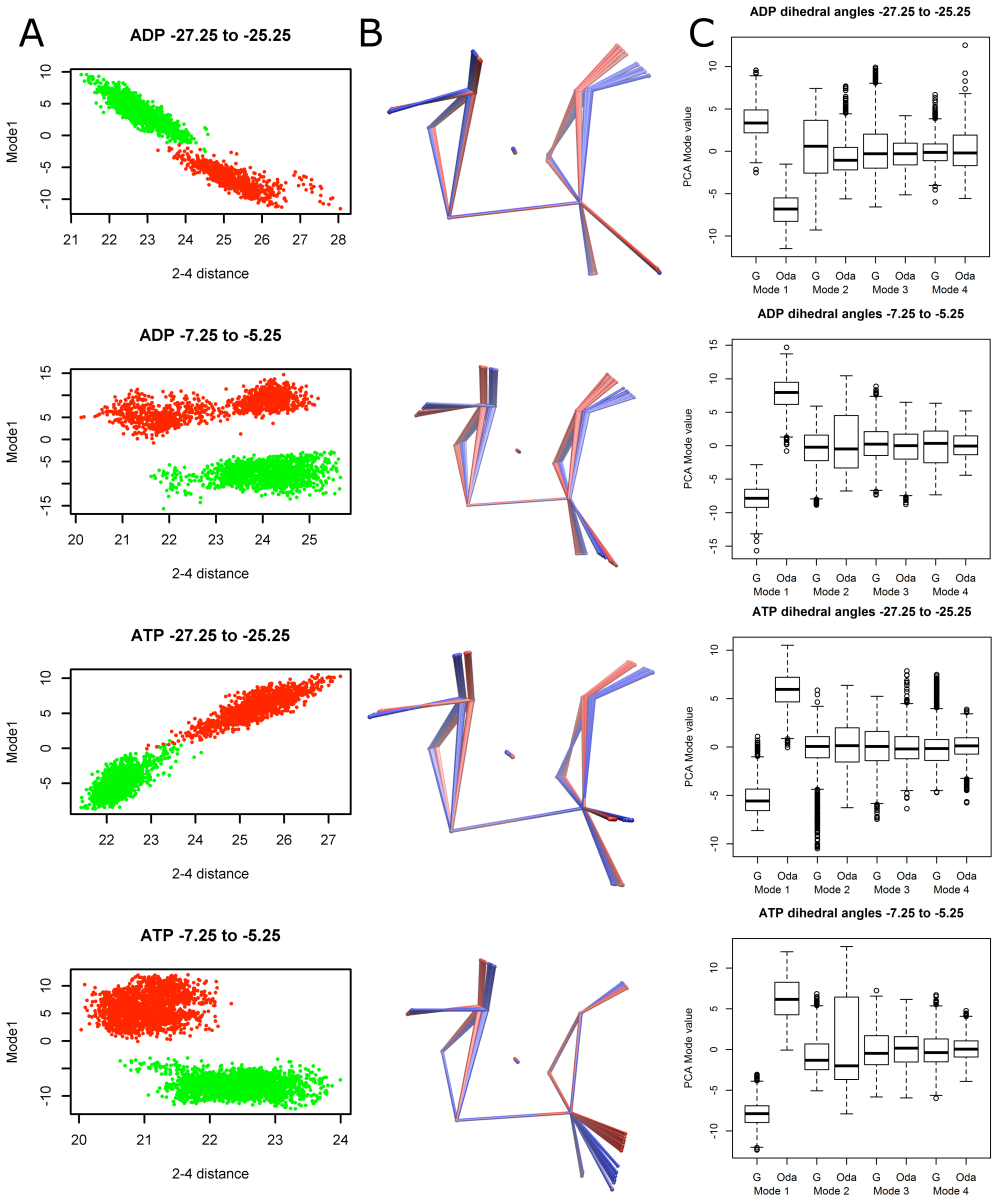

Figure S2: The lowest energy windows are locally equilibrated based on multiple, reversible transitions to the environment of neighboring windows. The MD trajectory from the lowest energy windows from each of the states simulated projected onto the 2 collective variables that we biased. The points are colored by time, starting from blue and going to red, sampling the trajectory every 10 ps. The dashed lines represent the midpoint between the lowest energy window and all adjacent windows.

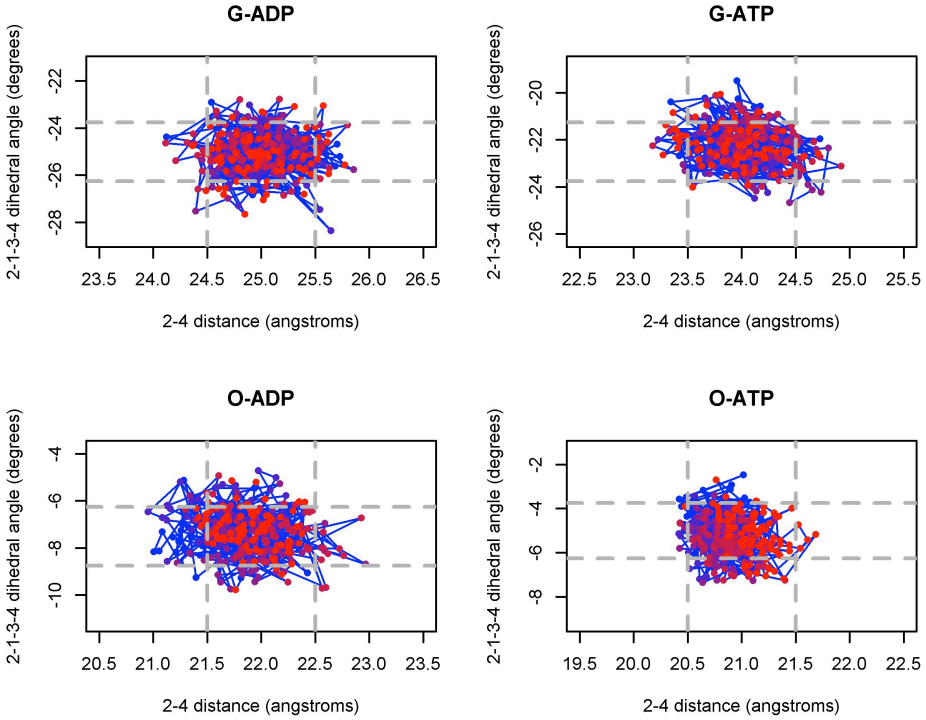

Figure S3: Integration of the area explored within a specific probability cutoff for each of the umbrella sampling simulation systems reveals that ADP-bound actin subunits are more conformationally flexible, particularly at high energy conformations.

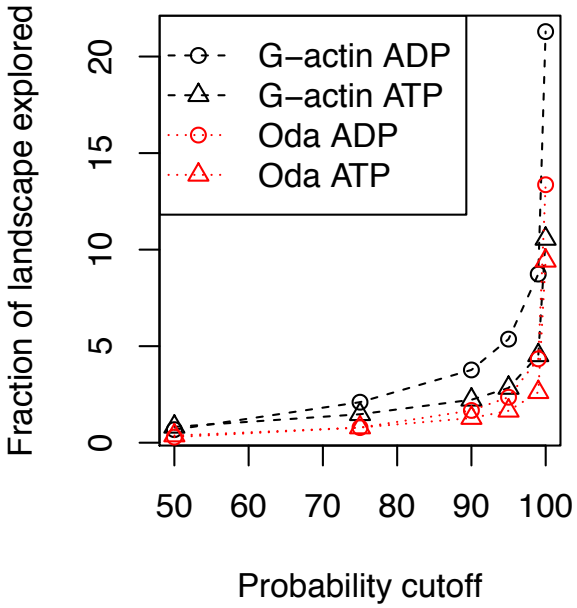

References

1. Splettstoesser, T., F. Noé, T. Oda, and J. C. Smith. 2009. Nucleotide-dependence of G-actin conformation from multiple molecular dynamics simulations and observation of a putatively polymerization-competent superclosed state. Proteins 76:353-364.
2. Saunders, M. G., and G. A. Voth. 2011. Water molecules in the nucleotide binding cleft of actin: Effects on subunit conformation and implications for ATP hydrolysis. J. Mol. Biol. 413:279-291.